Planning of Electric Vehicle Charging Stations Considering Fuzzy Selection of Second Life Batteries

Jiafeng Lin, Jing Qiu, *Senior Member, IEEE*, Yi Yang, *Graduate Student Member, IEEE*, and Weidong Lin

***Abstract*—The increasing sales of electric vehicles (EVs) in the market poses critical questions for the public on how to deal with millions of retired batteries (RBs). A number of studies have shown that second-life batteries (SLBs) from EVs usually have a considerable remaining capacity and hence still have additional utilization value. This article proposes a novel fuzzy inference system (FIS)-based planning framework for EV charging stations with wind, PV power, battery energy storage system and the utilization of SLBs (EVCS-WPE-SLBs system). In this framework, a narrowed and the most probable candidate node set for EVCS-WPE-SLBs system which makes the trade-off of several off-site factors from different fields that jointly determine the optimal planning results is obtained, including the installation and utilization requirements of SLBs, the transportation network features and power system properties. Numerical case studies are conducted on a coupled IEEE 33-bus distribution system and 25-node transportation system. According to the simulation results, the reasonable utilization of SLBs in the EVCS-WPE-SLBs system can reduce the total system cost while maintaining the normal operation of the system. Besides, a narrowed and most probable candidate node set not only reduces the search space and simplifies the optimization problem, but the results obtained are more practical according to the actual system conditions in real life.**

***Index Terms*—EV charging station planning, fuzzy inference system, renewable energy, battery energy storage system, second-life batteries (SLBs).**

NOMENCLATURE

Abbreviation

AEMO	Australian Energy Market Operator
BESS	Battery energy storage system
COE	Cost of electricity
CRF	Capital recovery factor
DOD	Depth of discharge
EVs	Electric vehicles
EVCSs	Electric vehicle charging stations
FIS	Fuzzy inference system
MFs	Membership functions
PV	Photovoltaic
RES	Renewable energy resources
SLBs	Second-life batteries
SLB-ESS	Second-life battery energy storage system
SOC	State of charge
SOH	State of health
WT	Wind turbine
WPE	Wind power, PV power, and energy storage system

Sets/Indices

ij, Ω^{DL}	Branches in distribution system
t, Ω^{T}	Index and set of time intervals
y, Ω^{Y}	Index and set of years
Ω^{BESS}	Set of mth-type BESS (fresh or SLBs)
Ω^{GN}	Set of grid-connected nodes
Ω^{KCS}	EVCS-WPE-SLBs candidate location set
Ω^{SLBs}	Probability set for the suitability of SLBs utilization at each node
Ω^{EVCS}	Probability set for the suitability of constructing an EVCS at each node

Parameters

β_T	Temperature coefficient of PV system
w_r	Rated output of the micro-WT
$\eta_{m,i}^{cha}, \eta_{m,i}^{dis}$	Charging/discharging efficiency of BESS
η_{PV}	Generation efficiency of PVs
$\zeta_{o,i,y}$, $\zeta_{u,i,y}$	Penalty costs for overestimation and underestimation available power
π^{PV}, π^{W}, $\pi_{m,y}^{BESS}$	Per-unit cost of PVs, micro-WT and mth-type BESS
$\pi_{ui,i,y}^{BESS}, \pi_{sal,i,y}^{BESS}$	Uninstallation and salvage cost of BESS
$\pi_{t,y}^{buy}, \pi_{t,y}^{sell}$	Electricity purchase price and feed-in tariff
$\pi_{y}^{MT,PV}, \pi_{y}^{MT,W}$	Maintenance cost of PVs and micro-WT
$\pi_{y}^{MT,ST}, \pi_{m,y}^{MT,BESS}$	Maintenance cost of substation and BESS
π_{y}^{envir}	Carbon cost coefficient
$\delta_{y}^{ST}, \delta_{y}^{BESS}$	Carbon emission intensity of the substation and BESS retirement
B_{ij}	Line susceptance at branch ij

Manuscript received 18 March 2023; revised 18 August 2023; accepted 9 October 2023. Date of publication 12 October 2023; date of current version 19 April 2024. This work was supported in part by the ARC Research Hub under Grant IH180100020, in part by the ARC Training Centre under Grant IC200100023, in part by the ARC linkage project under Grant LP200100056, and in part by the ARC under Grant DP220103881. Paper no. TPWRS-00351-2023. *(Corresponding author: Jing Qiu.)*

Jiafeng Lin, Jing Qiu, and Yi Yang are with the School of Electrical and Information Engineering, The University of Sydney, Sydney, NSW 2006, Australia (e-mail: jiafeng.lin@sydney.edu.au; qiujing0322@gmail.com; yyan9454@uni.sydney.edu.au).

Weidong Lin is with the Fujian Provincial Institute of Architectural Design and Research Company Ltd., Fuzhou 350001, China (e-mail: lwd@fjadi.com.cn).

Color versions of one or more figures in this article are available at https://doi.org/10.1109/TPWRS.2023.3324001.

Digital Object Identifier 10.1109/TPWRS.2023.3324001

CT Normal operation cell temperature of PVs

$E^{BESS}_{m,i,t,y,rated}$ Rated capacity of mth-type of BESS

K_p Peukert lifetime constant

$N^{\min}_{CS}, N^{\max}_{CS}$ Bounds of the required number of EVCS

$N^{total}_{100,m,i}$ Total number of cycles with 100% DOD

N_{days} Number of operating days in a year

N_0 Battery cycle parameter

P^{PV}_r Rated power of PVs

r Interest rate

T^C_{ref}, T_{amb} Cell reference temperature of PVs and ambient temperature

v_r, v_{in}, v_{out} Rated speed, cut-in speed and cut-out speed of micro-WT

y_k Lifecycle of kth component

$\overline{(\cdot)}(\cdot)$ Upper and lower bounds

D. Variables

$\theta_{i,t,y}$, $\theta_{j,t,y}$ Phase angle of bus i and bus j

$\mu^{dis}_{m,i,t,y}, \mu^{cha}_{m,i,t,y}$ Binary decision variables of BESS on simultaneous discharging and charging

$\mu_{\overline{\overline{K}}_n}(w)$ Membership functions of fuzzy sets $\overline{\overline{K}}$ under nth fuzzy rule

$\mu_{\overline{\overline{R_{Mn}}}}(\cdot)$ Fuzzy relationship between inputs and output

$\mu_{\overline{\overline{B}}^*}(y)$ Fuzzified result of fuzzy set $\overline{\overline{B}}^*$ of fuzzy variable y

ω Adaptation degree of fuzzy sets

$\lambda^{BESS}_{m,i,y}, \lambda^{BESS,retire}_{m,i,y}$ Decision variable of installation and retirement of mth-type of BESS

$\lambda^{PV}_{i,y}, \lambda^{W}_{i,y}, \lambda^{CS}_{i}$ Decision variable of installation of PVs, micro-WT and charging station at bus i

$\lambda^{ST,buy}_{i,t,y}, \lambda^{ST,sell}_{i,t,y}$ Decision variable of buying/selling electricity to the utility grid

$E^{BESS}_{m,i,t+1,y}, E^{BESS}_{m,i,t,y}$ Electricity stored in BESS at bus i

$I^r_{i,t,y}$ Solar radiation

$N^{PV}_{i,y}, N^{W}_{i,y}$ Number of PV and micro-WT

p^*_i Probability of constructing an EVCS at node i

$P^{dis}_{m,i,t,y}, P^{cha}_{m,i,t,y}$ Discharging and charging power of BESS

$P^{EV}_{i,t,y}$ EV charging demand at candidate bus i

$P^{PV}_{i,t,y}, P^{W}_{i,t,y}$ Actual output of PVs and micro-WT

$P^{PV,s}_{i,t,y}, P^{W,s}_{i,t,y}$ Scheduled output of PVs and micro-WT

$P^{buy}_{i,t,y}, P^{sell}_{i,t,y}$ Amount of electricity purchasing from or selling to the utility grid

$S_{ij,t,y}$ Power flow from bus i to bus j

$P^L_{i,t,y}$ Active load at bus i

$\Delta DOD_{m,i,t,y}$ Amount of DOD change in adjacent times

$N^{eqv,day}_{100,m,i,y}$ 100%-DOD equivalent BESS daily cycle number

$Loss^{cycle}_{m,i}(\%)$ Loss of BESS life cycles in percentage

$SOH_{m,i}(\%)$ Remaining SOH value of mth-type BESS

$SOH^{initial}_{m,i}(\%)$ Initial SOH value of mth-type BESS

$V_{i,t,y}$ Actual wind speed

I. Introduction

ELECTRIC vehicles (EVs) are gradually replacing traditional internal combustion vehicles due to the increasing environmental pressure (e.g., urban air pollution and climate change) and their potential in reducing carbon emissions. In 2020, global sales of EVs have increased by 43%, and more than 1.3 million EVs have been sold in China [1]. The accelerating market penetration of EVs has raised crucial questions for the industry on how to deal with millions of retired batteries from EVs that could be of great potential value. The retired batteries from EVs in China are estimated up to 1500–3300 thousand tons in 2040 [2]. Exploring additional utilization opportunities has been a research hotspot over recent years in order to realize the full potential of retired batteries. Currently, 70%–80% of state-of-health (SOH) is generally considered as the end-of-life of the EV batteries for their SOH can no longer satisfy the driving needs of the EV [3], [4], [5], [6]. Compared with fresh batteries, less maximum capacity, lower charging and discharging efficiency, shorter remaining cycle number are major drawbacks of the second-life batteries (SLBs) [7]. However, for those retired batteries which retain considerable SOH can be reused in other less-demanding fields after diagnosed, tested, sorted, and reassembled, such as microgrids, residential buildings, integrated renewable energy systems, etc. [1]. Regarding the costs of SLBs, it is believed that its cost should be 60% cheaper than fresh batteries [8]. Ref. [9] performed a detailed analysis of the price of SLBs and concluded that 50–70% price of fresh batteries is a relatively reasonable range. Therefore, the reasonable utilization of SLBs can not only reduce the costs of the system significantly but also improve the overall energy efficiency of the society.

Over the past decades, the planning of EV charging stations (EVCSs) with renewable energy resources (RES)-based generation and energy storage system has been well studied, including minimizing the system cost [10], minimizing the cost of electricity (COE) [11], multi-objective for minimizing the investment cost and energy losses [12], minimizing the COE and pollution emissions [13], maximizing annual profit and minimizing wind curtailment [14]. In these articles, the planning of EVCS is usually considered as a simple optimization problem. The optimal siting and sizing of the EVCS are obtained by considering only a few factors which can be modeled mathematically.

Battery reuse has been identified as a promising strategy for industry participants to improve the life cycle revenue of batteries and realize their full potential. Some automotive companies, including Nissan in the US, Toyota in Japan, BMW in Germany, Renault in the U.K., have launched projects for the application of SLBs from EVs. These projects target applications such as

renewables integration, backup power, peak shaving, residential energy storage [15], [16]. Additionally, the echelon utilization of retired batteries has attracted increasing interest among the researchers in recent years. Ref. [17] analyzed the utilization of a second life battery energy storage system (SLB-ESS) in home energy management application. In [7], a novel two-stage collaborative system planning model was proposed, which can realize the cyclic replacement of battery in a long-term planning period. The whole-life-cycle planning of BESS was analyzed in [18], where the BESS served the power grid regulation auxiliary service market and energy arbitrage market in its first and second lifespan, respectively.

The utilization of SLBs in the EVCSs is considered as another possible solution to realize the full potential of retired batteries. Companies such as EVgo, Connected Energy, Repsol are conducting round after round of research to integrate second-life batteries with EV charging stations. To our knowledge, only a few published papers discuss the utilization of SLBs in EVCSs. Ref. [19] proposed an operational planning framework for centralized charging stations integrated with PV and SLBs. A novel methodology was proposed in [20] to determine the optimal number of EVCSs in urban parking areas. Simulation results highlight the contribution of SLB-ESS in shaving the peak power demand due to the charging of EVs. In these works, the requirements for the installation and operation of SLBs are completely ignored.

A fuzzy inference system (FIS) is a computational framework for modeling uncertain and imprecise knowledge that cannot be expressed in traditional mathematical terms. It is a type of artificial intelligence technique that uses fuzzy logic to reason about vague information. A FIS can handle multiple variables as inputs at once and provides an advantage in terms of interpretability, allowing for a broader and more comprehensive decision-making process. This offers a more intuitive understanding of the system and makes it easier for decision-makers to interpret and act on the results. FIS has been widely applied in a variety of fields, from control systems, medical treatment, communications, signal processing, pattern recognition, decision making, and data analysis, etc. [21]. Ref. [22] proposed a novel approach for the classification of MRI images to diagnose Alzheimer's disease based on fuzzy inference system. Ref. [23] employed FIS to control the power flow in a hybrid system with EV and wind turbine. Ref. [24] used fuzzy inference-based control to regulate the SOC of a superconducting magnetic energy storage in a wind power system. In [25], FIS is adopted to design a smart charging management for EVs according to the battery state-of-charge (SOC), charging period and transformer loading. In summary, FIS is a very useful and effective methodology to take off-site factors into consideration and incorporate into the planning process.

In the above literature, it can be found that many of the previous work do not consider and incorporate the nonlinear, difficult-to-model joint effects of the off-site factors (e.g., environmental, political, social, or technological) that may lead to discrepancies between the obtained results and the actual situations into their planning models. For example, not all nodes in the system are suitable for the utilization of SLBs, the reduced capacity, shorter service lifespan, lower charging and discharging power and efficiency make specific requirements for the temperature, humidity, policy supports, and environmental pollution levels at their installation locations. In other words, whether the utilization of SLBs is feasible needs to take into account many off-site condition factors. Moreover, the number of EVs, the relative importance or preference of a node, the distance between neighboring nodes, the maximum load capacity of the power grid, and the development of public transportation in this region may also jointly influence the planning of EVCSs. Therefore, a novel planning framework that can take these off-site factors into consideration for the EVCS with wind energy, PV power, energy storage system and SLBs (EVCS-WPE-SLBs system) is urgently needed.

To fill the existing research gaps, this article proposes a novel planning framework for EVCS-WPE-SLBs system that incorporates the complex, difficult-to-model joint effects of several off-site factors into the planning process. The major contributions in this article can be summarized as follows:

1) We propose a novel fuzzy inference system-based comprehensive candidate location selection method for the planning of EVCSs and the utilization of SLBs. A narrowed and the most probable candidate location set for EVCS-WPE-SLBs system is obtained considering several off-site factors which jointly determine the optimal planning results. These factors include the installation and utilization requirements of SLBs, the features of transportation network, and power system properties.
2) We consider those off-site condition factors which affect the echelon utilization of SLBs and incorporate them into the planning process. Compared with the existing research on SLB applications, the method proposed in this article is more realistic according to practical system conditions because more possible factors under actual situations are taken into consideration.
3) We propose a novel optimization planning framework for EVCS considering the optimal configuration of PV, wind power, energy storage system and the echelon utilization of second-life batteries simultaneously. The optimal planning results are obtained considering the trade-off among several decisive factors. These factors effectively capture the complexities of real-world planning for the EVCS-WPE-SLBs system, thereby producing more realistic and useful results in terms of where the charging stations are most needed and how the capacity should be optimally configured. Numerical case studies are conducted to demonstrate the economic benefits of the proposed planning method.

The remainder of this article is organized as follows. In Section II, the overview of the proposed planning framework is presented. Section III introduces the proposed fuzzy inference-based candidate node set selection method, where the implementation processes of the method are discussed in detail. Section IV provides the mathematical models of the optimization problem. Case studies are presented in Section V to verify the effectiveness and scalability of the proposed method. Finally, Section VI concludes this article.

II. Overview of the Proposed FIS-Based Planning Framework

As aforementioned, in real-world planning of the EVCS-WPE-SLBs system, the final decision-making should be based on the joint effect of several off-site factors in terms of environmental, political, social and technological aspects. However, the relationship among these factors and their joint impact is highly complex and cannot be precisely described by mathematical models.

The FIS uses fuzzy logic to make decisions based on ambiguous information. Compared to other methods of modeling uncertain and imprecise knowledge, such as stochastic optimization and information gap decision theory, the FIS does not require a comprehensive mathematical model. This makes it more flexible and adaptable in handling complex nonlinear functions, especially when the relationship among all input factors is imprecise or uncertain, and where traditional mathematical models may not be appropriate.

In a fuzzy inference system, the decision-making process consists of three steps: fuzzification, rules evaluation, and defuzzification. Fuzzification is the step that converts the inputs (e.g., two inputs x and y) into fuzzy sets, denoted by $\overline{\overline{A}}$ and $\overline{\overline{B}}$, respectively. This can be done using membership functions (MFs) that assign a degree of membership to each input variable, determining how much each variable contributes to the overall result, as shown in (1). The obtained MFs are then used to fuzzify the input variables based on a set of fuzzy rules table using Mamdani fuzzy inference algorithm. Its fuzzy implication relationship is straightforwardly defined, which can be obtained by taking the Cartesian product of the fuzzy sets to a minimal value, as shown in (2)–(3). Finally, through defuzzification, the fuzzy output is converted into a crisp value suitable for direct decision making.

$$\begin{cases} \mu_{\overline{\overline{A}}}(x) = [(x-a)/(b-a)]a \le x \le b \\ \mu_{\overline{\overline{A}}}(x) = [(c-x)/(c-b)]b \le x \le c \\ \mu_{\overline{\overline{B}}}(y) = [(y-u)/(v-u)]u \le y \le v \\ \mu_{\overline{\overline{B}}}(y) = [(w-y)/(w-v)]v \le y \le w \end{cases} \tag{1}$$

$$\mu_{\overline{\overline{R_M}}}(x,y) = \mu_{\overline{\overline{A}}}(x) \wedge \mu_{\overline{\overline{B}}}(y) \tag{2}$$

$$\begin{aligned} \mu_{\overline{\overline{B}}^*}(y) &= \underset{x \in X}{\vee} \left\{ \mu_{\overline{\overline{A}}^*}(x) \wedge [\mu_{\overline{\overline{A}}}(x) \wedge \mu_{\overline{\overline{B}}}(y)] \right\} \\ &= \underset{x \in X}{\vee} \left\{ [\mu_{\overline{\overline{A}}^*}(x) \wedge \mu_{\overline{\overline{A}}}(x)] \wedge \mu_{\overline{\overline{B}}}(y) \right\} \\ &= \omega \wedge \mu_{\overline{\overline{B}}}(y) \end{aligned} \tag{3}$$

where $\mu_{\overline{\overline{A}}}(x)$ and $\mu_{\overline{\overline{B}}}(y)$ are the membership functions; a, b, c, u, v and w are the parameters that define the shapes of the triangular membership function; $\overline{\overline{A}}^*$, $\overline{\overline{A}}$ and $\overline{\overline{B}}$ are the fuzzy sets, $\mu_{\overline{\overline{B}}^*}(y)$ is the fuzzified result of set $\overline{\overline{B}}^*$, ω is the maximum value of $\mu_{\overline{\overline{A}}^*}(x) \wedge \mu_{\overline{\overline{A}}}(x)$, defined as the adaptation degree of $\overline{\overline{A}}^*$, $\overline{\overline{A}}$. Note that the selection of MFs is related to the expert experience, the knowledge and cognition of the decision maker, and can vary based on different planning scenarios.

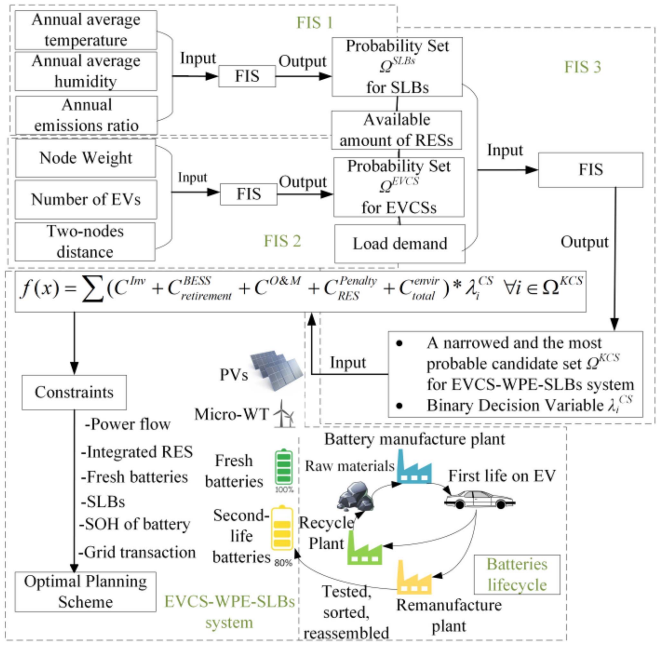

Fig. 1. Proposed planning framework.

Considering the advantages of the FIS, this article proposed a novel FIS-based framework for the comprehensive planning of the EVCS-WPE-SLBs system, as illustrated in Fig. 1.

The proposed planning framework incorporates a wide array of practical system characteristics. Eight off-site factors from different aspects are taken into consideration in our model. Three of these factors are related to environment: annual average temperature, annual average humidity and annual emissions ratio. These factors are critical for understanding and reflecting the installation and application requirements of the SLBs. Another three factors are related to the transportation system features: the node weights, the number of EVs and the distance between neighboring nodes. These factors are crucial for reflecting the preference of constructing an EVCS at a particular transportation node within the system. Moreover, the load demand and the amount of available RESs, two factors from a power system perspective, are also considered. These factors are crucial for accounting for the suitability of the RES-based generation application. By taking into account the joint effect of these practical off-site system conditions, the proposed planning framework can better capture the complexities of real-world planning of the EVCS-WPE-SLBs system, thereby producing more realistic and useful results for the siting and sizing of EVCSs.

First, a probability set Ω^{SLBs} for the most suitable locations to utilize SLBs in the system is obtained by a FIS. Similarly, a probability set Ω^{EVCS} that contains the information about the most appropriate locations for EVCSs in the transportation network is derived from another FIS. Then, a narrowed and most probable candidate set Ω^{KCS} for EVCS-WPE-SLBs system is determined by considering local load demand, available RESs and these two probability sets. Next, the narrowed candidate set Ω^{KCS} and a binary decision variable λ_i^{CS} are passed to the optimization problem, which aims to minimize the total system cost of the

EVCS-WPE-SLBs system. The system investment cost, system operation and maintenance cost, overestimated and underestimated penalty costs of RESs and environmental penalty cost are considered. Finally, the optimal siting and sizing of the EVCS-WPE-SLBs are determined under normal power system operation constraints. The detailed implementation steps and mathematical models are presented and discussed in Section III and Section IV, respectively.

III. Proposed FIS-Based Candidate Node Set Selection Method

A. SLBs Candidate Installation Locations Selection

The utilization of second-life batteries is increasingly factored into power system planning due to their significant economic, environmental and social benefits. However, not all nodes in the system are suitable for installing SLBs. Off-site factors such as climate conditions, regional policy support, safety considerations and economic benefits can also influence the feasibility of SLB applications in a given region. For example, the milder the climate conditions, the greater the regional policy support, the higher the safety considerations, and the larger economic benefits, the more suitable a location is for SLB utilization.

Generally speaking, batteries initially degrade at a relatively slow and stable rate. However, after passing the aging knee point, the performance of the BESS experiences a sudden and rapid increase in the degradation rate, especially in the case of SLBs. The major shortcomings of SLBs, such as reduced capacity, shorter service lifespan, lower charging and discharging efficiency necessitate specific requirements for the temperature, humidity and environmental pollution levels at their installation locations. In general, higher temperatures can accelerate battery degradation while lower temperatures will reduce battery performance; a higher humidity level can increase the risk of corrosion while lower humidity level may cause the battery to dry out, both of which will shorten its lifespan. Moreover, selecting proper locations for SLBs that minimizes the risk of environmental pollution is important.

Therefore, how to make the decision based on the joint effect of these off-site factors which cannot be mathematically modelled is a critical problem. To solve this problem, a novel three-input-one-output fuzzy inference system is proposed. This approach enables the calculation of a suitable probability set, denoted as Ω^{SLBs}, for the application of SLBs at each node in the system, accounting for the trade-off between three decisive factors. The detailed process of the proposed fuzzy inference system method is shown below.

The fuzzy rules proposed in this article are given in Table I. Due to page limits, 5 of them are listed. For example, if the temperature and humidity are more proper (M), and the annual environmental emissions ratio is lower (L), a higher (H) probability for the application of SLBs at this node.

Define X {temperature}, Y {humidity} and Z {emissions ratio} are fuzzy variables with fuzzy sets $\overline{\overline{L}}^*$, $\overline{\overline{L}}_1$, $\overline{\overline{L}}_2 \ldots \overline{\overline{L}}_n$, $\overline{\overline{M}}^*$, $\overline{\overline{M}}_1$, $\overline{\overline{M}}_2 \ldots \overline{\overline{M}}_n$, $\overline{\overline{N}}^*$, $\overline{\overline{N}}_1$, $\overline{\overline{N}}_2 \ldots \overline{\overline{N}}_n$, respectively. O {probability} is the output variable with fuzzy sets $\overline{\overline{P}}^*$, $\overline{\overline{P}}_1$, $\overline{\overline{P}}_2 \ldots \overline{\overline{P}}_n$,

FIS-based SLB candidate installation locations selection.

1: **Initialization:** Initialize and fuzzify the values of three off-site factors: annual average temperature (°C), annual average humidity (%) and the annual environmental emissions ratio (%) as the inputs of the FIS.
2: **Determine the value range of input and output variables:** Temperature and humidity are divided into five levels: Low (L), Medium-Low (ML), Medium (M), Medium-High (MH) and High (H) in the ranges of [10,30] and [0%,100%], respectively. The annual environmental emissions ratio is categorized into three levels in the range of [0%,100%]: Low (L), Middle (M) and High (H). The output of FIS is divided into five levels in the range of [0,1]: Low (L), Medium-Low (ML), Medium (M), Medium-High (MH), High (H), which represents the probability that SLBs are suitable for each location (node).
3: **Select proper fuzzy Membership functions, determine the customized fuzzy rules table, and fuzzify the inputs:** Select appropriate types of MFs for the variables, which mapping each input value to a degree of membership in each relevant fuzzy set based on the shape of the MF. A rules table which consists of 75 rules in total is proposed. The Mamdani fuzzy inference method is used to obtain fuzzy sets under the proposed fuzzy rules table, as shown in (4)–(5).
4: **Defuzzify the output variable and obtain the results:** Using the Centroid defuzzification method, the suitability probability for the application of SLBs at each node is converted into a crisp value in the range of [0,1]. By ranking the probabilities from highest to lowest, a probability set Ω^{SLBs} for SLBs candidate locations can be obtained.

TABLE I
Five Example Fuzzy Rules for SLBs

Annual average temperature	Annual average humidity	Annual environmental emissions ratio	Probability that suitable for application of SLBs
L	L	H	L
ML	ML	H	ML
M	M	L	H
MH	MH	M	M
H	H	H	L

which represents the probability that is suitable to install and utilize SLBs at each node. $\overline{\overline{R_{Mn}}}(X, Y, Z, O)$ represents the fuzzy rules that relate the inputs X, Y, Z and output O, where n is the number of rules.

$$\mu_{\overline{\overline{R_{Mn}}}}(x, y, z, o) = \mu_{\overline{\overline{L_n}}}(x) \wedge \mu_{\overline{\overline{M_n}}}(y) \wedge \mu_{\overline{\overline{N_n}}}(z) \vee \mu_{\overline{\overline{P_n}}}(o)$$
$$\forall x \subset \{[10, 30]\} y \subset \{[0, 1]\} z \subset \{[0, 1]\} \mathrm{o} \subset \{[0, 1]\} \quad (4)$$

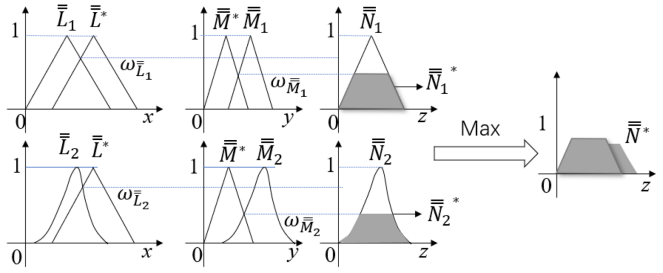

Fig. 2. Mamdani inference process.

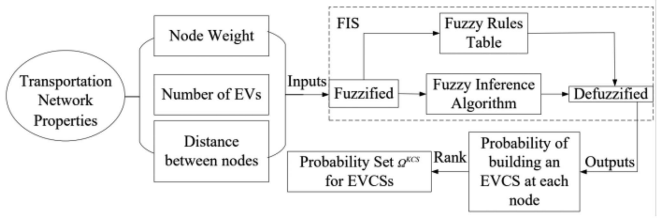

Fig. 3. Process of the proposed FIS method for EVCS.

where $\mu_{\overline{\overline{L_n}}}(x)$, $\mu_{\overline{\overline{M_n}}}(y)$, $\mu_{\overline{\overline{N_n}}}(z)$ and $\mu_{\overline{\overline{P_n}}}(o)$ represent the selected MFs (where Gaussian MFs are used in this case) of fuzzy sets $\overline{\overline{L}}$, $\overline{\overline{M}}$, $\overline{\overline{N}}$ and $\overline{\overline{P}}$ under *n*th fuzzy rules, respectively.

Then, the fuzzy output sets {probability} from the rules are combined using the maximum operator to obtain the overall fuzzy output set, as shown in (5).

$$\begin{aligned}
&\mu_{\overline{\overline{P}}^*}(o)\\
&= [\mu_{\overline{\overline{L}}^*}(x) \wedge \mu_{\overline{\overline{M}}^*}(y) \wedge \mu_{\overline{\overline{N}}^*}(z)] \wedge [\mu_{\overline{\overline{R_{M1}}}}(x,y,z,o) \vee \ldots\\
&\ldots \vee \mu_{\overline{\overline{R_{Mn}}}}(x,y,z,o)] \forall x \subset X, y \subset Y, z \subset Z\\
&= \{[\mu_{\overline{\overline{L}}^*}(x) \wedge \mu_{\overline{\overline{M}}^*}(y) \wedge \mu_{\overline{\overline{N}}^*}(z)] \wedge \mu_{\overline{\overline{R_{M1}}}}(x,y,z,o)\}\\
&\vee \{[\mu_{\overline{\overline{L}}^*}(x) \wedge \mu_{\overline{\overline{M}}^*}(y) \wedge \mu_{\overline{\overline{N}}^*}(z)] \wedge \mu_{\overline{\overline{R_{M2}}}}(x,y,z,o)\} \ldots\\
&\ldots \vee \{[\mu_{\overline{\overline{L}}^*}(x) \wedge \mu_{\overline{\overline{M}}^*}(y) \wedge \mu_{\overline{\overline{N}}^*}(z)] \wedge \mu_{\overline{\overline{R_{Mn}}}}(x,y,z,o)\}\\
&= \mu_{\overline{\overline{P_1}}^*}(o) \vee \mu_{\overline{\overline{P_2}}^*}(o) \vee \ldots \vee \mu_{\overline{\overline{P_n}}^*}(o) \qquad (5)
\end{aligned}$$

where $\mu_{\overline{\overline{P_n}}^*}(o)$ is the fuzzy sets obtained under *n*th fuzzy rule.

The fuzzy inference implementation process can be easily explained graphically, as indicated in Fig. 2(for a case with only two rules).

Note that the obtained Ω^{SLBs} only contains the probabilities suitable for the utilization of SLBs at each node in the system. The final decision on the installation location of the SLBs in the EVCS-WPE-SLBs system needs to consider the characteristics of both the transportation and power systems as well, as described in Section B and C.

B. EV Charging Station Node Set Selection

As aforementioned, similarly, a great number of off-site factors will jointly affect the planning of EVCSs. For example, nodes with higher weight may be prioritized when planning EVCSs to ensure drivers have access to charging infrastructure in areas where they are more likely to need it; areas with more EVs may require a greater number of charging stations to meet the needs of drivers; regions with robust public transportation infrastructure may see reduced demand for EVCSs; and the larger the distance between neighboring nodes, the greater the number of EVCSs may be required. Therefore, how to make the decision based on the trade-off of these factors is a critical problem. To address this problem, a three-input-one-output FIS is proposed. It considers three features from transportation networks: the node weights, the number of EVs and the distance between neighboring nodes.

TABLE II
FIVE EXAMPLE FUZZY RULES FOR EVCSS

Node weight	Number of EVs	Distance between neighboring nodes	Probability of building an EVCS
L	L	L	L
ML	ML	L	ML
M	M	M	M
MH	MH	M	MH
H	H	H	H

The process of the proposed FIS is illustrated in Fig. 3.

First, the node weights and the number of EVs are initialized as the inputs of FIS and categorized into five levels: Low (L), Medium-Low (ML), Medium (M), Medium-High (MH) and High (H), within the range of $[W_{\min}, W_{\max}]$ and $[N_{ev,\min}, N_{ev,\max}]$, respectively. The distance between neighboring nodes is divided into three categories within the range of $[D_{\min}, D_{\max}]$: Low (L), Middle (M) and High (H). The output of the FIS, representing the probability that a charging station is constructed at each node, is divided into five levels within the range of [0,1]: Low (L), Medium-Low (ML), Medium (M), Medium-High (MH), High (H). Next, based on the customized fuzzy rules table (Table II) and MFs, the fuzzy outputs are derived using the Mamdani inference algorithm (6)–(7). Using the centroid defuzzification method, the probabilities for constructing an EVCS at each node are converted to crisp values. After ranking these probabilities from highest to lowest, the required number of nodes with high probability is selected to form the candidate node set Ω^{EVCS}. At this point, a probability set for appropriately locating the EVCSs in the transportation network is obtained.

Due to page limits, only 5 of 75 fuzzy rules are listed in Table II. For example, the larger the node weight, the greater the number of EVs at this node, and the larger the distance between its neighboring nodes, the higher the probability of constructing an EVCS at this node.

Define $\overline{\overline{\mathrm{U}}}^*$, $\overline{\overline{\mathrm{U}}}_1$, $\overline{\overline{\mathrm{U}}}_2 \ldots \overline{\overline{\mathrm{U}}}_\mathrm{n}$, $\overline{\overline{\mathrm{V}}}^*$, $\overline{\overline{\mathrm{V}}}_1$, $\overline{\overline{\mathrm{V}}}_2 \ldots \overline{\overline{\mathrm{V}}}_\mathrm{n}$, $\overline{\overline{\mathrm{W}}}^*$, $\overline{\overline{\mathrm{W}}}_1$, $\overline{\overline{\mathrm{W}}}_2 \ldots \overline{\overline{\mathrm{W}}}_\mathrm{n}$ and $\overline{\overline{\mathrm{S}}}^*$, $\overline{\overline{\mathrm{S}}}_1$, $\overline{\overline{\mathrm{S}}}_2 \ldots \overline{\overline{\mathrm{S}}}_\mathrm{n}$ are the fuzzy sets over domains X' {the node weight}, Y' {the number of EVs}, Z' {distance between neighboring nodes} and O' {probability of constructing the EVCS at each node}, respectively. $\overline{\overline{\mathrm{R_{Mn}}}}(\mathrm{X}', \mathrm{Y}', \mathrm{Z}', \mathrm{O}')$ represents the fuzzy implication relationship between $\overline{\overline{\mathrm{U}}}_\mathrm{n}$, $\overline{\overline{\mathrm{V}}}_\mathrm{n}$, $\overline{\overline{\mathrm{W}}}_\mathrm{n}$ and $\overline{\overline{\mathrm{S}}}_\mathrm{n}$, where *n* is the number of rules.

$$\mu_{\overline{\overline{R_{Mn}}}}(x', y', z', o') = \mu_{\overline{\overline{U_n}}}(x') \wedge \mu_{\overline{\overline{V_n}}}(y') \wedge \mu_{\overline{\overline{W_n}}}(z') \vee \mu_{\overline{\overline{S_n}}}(o')$$

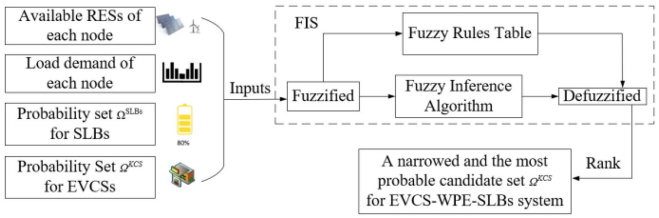

Fig. 4. Process of the proposed FIS method for EVCS-WPE-SLBs.

$$\forall x' \subset \{[W_{\min}, W_{\max}]\}, y' \subset \{[N^{ev}_{\min}, N^{ev}_{\max}]\} z' \subset \{[D_{\min}, D_{\max}]\} o' \subset \{[0,1]\} \quad (6)$$

where $\mu_{\overline{\mathrm{U}}_n}(x')$, $\mu_{\overline{\mathrm{V}}_n}(y')$, $\mu_{\overline{\mathrm{W}}_n}(z')$ and $\mu_{\overline{\mathrm{S}}_n}(o')$ represent the selected MFs of fuzzy sets $\overline{\mathrm{U}}$, $\overline{\mathrm{V}}$, $\overline{\mathrm{W}}$ and $\overline{\mathrm{S}}$ under *n*th fuzzy rules, respectively.

$$\begin{aligned}
&\mu_{\overline{S}^*}(o') \\
&= [\mu_{\overline{U}^*}(x') \wedge \mu_{\overline{V}^*}(y') \wedge \mu_{\overline{W}^*}(z')] \wedge [\mu_{\overline{R_{M1}}}(x', y', z', o') \vee \dots \\
&\dots \vee \mu_{\overline{R_{Mn}}}(x', y', z', o')] \forall x' \subset X', y' \subset Y', z' \subset Z' \\
&= \{[\mu_{\overline{U}^*}(x') \wedge \mu_{\overline{V}^*}(y') \wedge \mu_{\overline{W}^*}(z')] \wedge \mu_{\overline{R_{M1}}}(x', y', z', o')\} \\
&\vee \{[\mu_{\overline{U}^*}(x') \wedge \mu_{\overline{V}^*}(y') \wedge \mu_{\overline{W}^*}(z')] \wedge \mu_{\overline{R_{M2}}}(x', y', z', o')\} \dots \\
&\dots \vee \{[\mu_{\overline{U}^*}(x') \wedge \mu_{\overline{V}^*}(y') \wedge \mu_{\overline{W}^*}(z')] \wedge \mu_{\overline{R_{Mn}}}(x', y', z', o')\} \\
&= \mu_{\overline{S_1}^*}(o') \vee \mu_{\overline{S_2}^*}(o') \vee \dots \vee \mu_{\overline{S_n}^*}(o') \qquad (7)
\end{aligned}$$

where $\mu_{\overline{\mathrm{S}}_n^*}(\mathrm{o}')$ is the output fuzzy sets obtained under *n*th fuzzy rule.

C. Candidate Node Set Selection for EVCS-WPE-SLBs System

In previous sections, two probability sets Ω^{SLBs} and Ω^{EVCS} are obtained, which consider the installation and utilization requirements of SLBs, and the transportation features, respectively. However, some off-site factors from the power system perspective, such as the available amount of RESs and the distance to demand side, can also affect the planning of the EVCS-WPE-SLBs system and should be taken into account at the planning stage as well. For example, the EVCS-WPE-SLBs system should ideally be located close to renewable sources (e.g., wind and solar) and areas with high demand to minimize transmission loss. Therefore, we propose a four-input-one-output FIS to model the trade-off between these factors whose joint effect is imprecise and difficult to express mathematically. The process is illustrated in Fig. 4.

Following the similar steps discussed in Section III, Part B, after fuzzifying, fuzzy inference evaluation and defuzzifying, the joint effect of the four factors: the available RESs ratio (%) at each node, load demand (kW) on each node, probability that SLBs is suitable to install at each node (Ω^{SLBs}) and the probability for building EVCS at each transportation node (Ω^{EVCS}), are characterized and converted into crips values, which represent the probability of constructing an EVCS-WPE-SLBs at each node.

TABLE III
FIVE EXAMPLE FUZZY RULES FOR EVCS-WPE-SLBS SYSTEM

Available RESs ratio (%)	Load demand (kW)	Suitable probability set Ω^{SLBs}	Suitable probability set Ω^{EVCS}	Probability of building EVCS-WPE-SLBs system
L	L	L	L	L
ML	ML	ML	ML	ML
M	M	M	M	M
MH	MH	MH	MH	MH
H	H	H	H	H

Finally, by ranking the probabilities from highest to lowest, we can obtain a narrowed and the most probable candidate node set Ω^{KCS} for the EVCS-WPE-SLBs system. This candidate set is determined based on the trade-off of several off-site factors, including those from the suitability of SLBs' echelon utilization aspect, the transportation perspective and power system properties.

Due to page limits, only 5 of the 225 fuzzy rules are listed in Table III. For example, the closer (L) a node is to the RESs, the higher (H) the demand on this node, the greater (H) the probability that is suitable for installing SLBs and constructing EVCS at this node, the larger (H) the probability for EVCS-WPE-SLBs is located at this node.

IV. MATHEMATICAL MODELS

The models obtained by the proposed fuzzy inference-based candidate node set selection method can be written as (8)–(10).

The degree of membership of *P* (probability) in each fuzzy set is computed using the minimum operator. Then, the fuzzy output sets from each fuzzy rule are combined using the maximum operator to obtain the overall fuzzy output set $\mu(P)$, as shown in (8).

$$\begin{aligned}
&\mu(P) = \\
&\max(\min(\mu_L(RESs), \mu_L(Load), \mu_L(\Omega^{SLBs}), \mu_L(\Omega^{EVCS})), \\
&\min(\mu_L(RESs), \mu_L(Load), \mu_L(\Omega^{SLBs}), \mu_{ML}(\Omega^{EVCS})), \dots \\
&\dots \min(\mu_H(RESs), \mu_H(Load), \mu_H(\Omega^{SLBs}), \mu_H(\Omega^{EVCS})))
\end{aligned} \quad (8)$$

where $\mu_x(RESs)$, $\mu_x(Load)$, $\mu_x(\Omega^{SLBs})$, $\mu_x(\Omega^{EVCS})$ are respectively the fuzzy input sets of available RESs ratio, load demand, suitable probability set Ω^{SLBs} and suitable probability set Ω^{EVCS}.

The probability of building an EVCS at each node can be obtained in crisp value, as calculated by (9).

$$p^*(probability) = \frac{\int p \cdot \mu(P) dp}{\int \mu(P) dp} = \frac{\sum_i p_i \cdot \mu(P_i)}{\sum_i \mu(P_i)} \quad (9)$$

where p^* is the probability of constructing an EVCS at each node in the distribution system; p_i is a discrete value in the universe of discourse *P*, which contains all the probabilities; $\mu(P_i)$ denotes the membership grade of the fuzzy set for probability of node *i*. Equation (9) represents the center of gravity of the fuzzy set as a crisp value by calculating the weighted average of the output variable corresponding to the membership grades of the fuzzy set.

Rank the probabilities from the highest to the lowest. Then, select the required number of nodes with the highest probability to form the candidate node set Ω^{KCS}, which is one of the important variables passed to the optimization problem.

$$\Omega^{KCS} = Rank(p_1^*, p_2^*, p_3^* \dots p_i^*) \forall i \in \{distribution\ nodes\} \tag{10}$$

Equations (11)–(13) define four binary decision variables $\lambda_i^{CS}, \lambda_{i,y}^{PV}, \lambda_{i,y}^{W}$ and $\lambda_{m,i,y}^{BESS}$. These variables are passed to the optimization problem to indicate the installation status of EVCSs, PVs, micro-WTs and BESSs at node *i* in the *y*th year, respectively. A value of 1 indicates the installation, while 0 indicates otherwise. We assume that these renewable energy facilities can only be installed when a charging station is constructed at candidate node *i*. This is a reasonable assumption for the potential benefits of reducing electricity transmission losses and infrastructure costs.

$$\lambda_i^{CS} = \begin{cases} 1 \\ 0 \end{cases} \quad \forall i \in \Omega^{KCS} \tag{11}$$

$$\lambda_{m,i,y}^{BESS}, \lambda_{i,y}^{W}, \lambda_{i,y}^{PV} \le \lambda_i^{CS} \forall i \in \Omega^{KCS}, y \in \Omega^{Y}, m \in \Omega^{BESS} \tag{12}$$

$$N_{CS}^{\min} \le \sum \lambda_i^{CS} \le N_{CS}^{\max} \forall i \in \Omega^{KCS} \tag{13}$$

The objective is to minimize the total cost of the whole EVCS-WPE-SLBs system, as shown in (14). The total duration of the system planning is up to *Y* years.

$$\min \pi = CRF \times \left[C_{total}^{RES\&BESS} + C_{total}^{O\&M} + C_{total}^{envir} \right] \tag{14}$$

where $C_{total}^{RES\&BESS}$, $C_{total}^{O\&M}$, C_{total}^{envir} represent the total cost of renewable energy and BESS, operation and maintenance cost of all system facilities and system environmental penalty cost, respectively. CRF is the capital recovery factor, calculated by (15); *r* is the interest rate; y_k is the lifecycle of *k*th component.

$$CRF_K = \frac{r \times (1+r)^{y_k}}{(1+r)^{y_k} - 1} \forall k \in \{W, PV, BESS\} \tag{15}$$

The total cost of renewable energy facilities and BESS includes the investment cost of PV panels, micro-WT and BESS, as well as the retirement cost of BESS, as shown in (16).

$$\begin{aligned} C_{total}^{RES\&BESS} &= C_{Inv}^{RES} + C_{Inv}^{BESS} + C_{retirement}^{BESS} \\ &= \sum_{i \in \Omega^{KCS}} \left(\pi^{PV} \cdot \lambda_{i,y}^{PV} \right) + \sum_{i \in \Omega^{KCS}} \left(\pi^{W} \cdot \lambda_{i,y}^{W} \right) \\ &+ \sum_{m \in \Omega^{BESS}} \sum_{i \in \Omega^{KCS}} \left(\pi_{m,y}^{BESS} \cdot \overline{E_{m,i,t,y}^{BESS}} \cdot \lambda_{m,i,y}^{BESS} \right) \\ &+ \sum_{m \in \Omega^{BESS}} \sum_{i \in \Omega^{KCS}} \left(\pi_{ui,i,y}^{BESS} - \pi_{sal,i,y}^{BESS} \right) \\ &\cdot \left(\overline{E_{m,i,t,y}^{BESS}} \cdot \lambda_{m,i,y}^{BESS,retire} \right) \end{aligned} \tag{16}$$

where π^{PV}, π^{W} and $\pi_{m,y}^{BESS}$ represent the per-unit cost of PV, micro-WT and *m*th-type BESS (fresh or SLBs), respectively; $\pi_{ui,i,y}^{BESS}$ and $\pi_{sal,i,y}^{BESS}$ respectively define the uninstallation cost and salvage cost of the BESS when the battery installed at bus *i* is determined to be retired; $\overline{E_{m,i,t,y}^{BESS}}$ is the maximum capacity of BESS; $\lambda_{m,i,y}^{BESS,retire}$ is another decision variable that determine the retirement of *m*th-type BESS; Ω^{BESS} is the set of *m*th-type BESS (fresh or SLBs).

The system operation and maintenance cost consists of the costs for purchasing and selling electricity with the substation, maintaining the substation, renewable energy devices and the BESS. Besides, to properly model the significant impacts on power system operation due to the great uncertainties of RESs, the overestimated and underestimated penalty costs of the actual available RES power are introduced, as shown in (17).

$$\begin{aligned} C_{total}^{OM} &= C_{ST}^{O\&M} + C_{RES}^{Mt} + C_{BESS}^{Mt} + C_{RES}^{oves} + C_{RES}^{unes} \\ &= \sum_{y \in \Omega^{Y}} \sum_{t \in \Omega^{T}} \left\{ \sum_{i \in \Omega^{GN}} [(\pi_{t,y}^{buy} + \pi_{y}^{Mt,ST}) \cdot P_{i,t,y}^{buy} - \pi_{t,y}^{sell} \cdot P_{i,t,y}^{sell}] \Delta t \right. \\ &+ \sum_{i \in \Omega^{KCS}} \pi_{y}^{MT,W} \cdot \lambda_{i,y}^{W} + \sum_{i \in \Omega^{KCS}} \pi_{y}^{MT,PV} \cdot \lambda_{i,y}^{PV} \\ &+ \sum_{m \in \Omega^{BESS}} \sum_{i \in \Omega^{KCS}} \pi_{m,y}^{MT,BESS} \cdot \left(\lambda_{m,i,y}^{BESS} - \lambda_{m,i,y}^{BESS,retire} \right) \\ &+ \sum_{i \in \Omega^{KCS}} \xi_{w,o,i,y} \cdot max \left(0, P_{i,t,y}^{W} - P_{i,t,y}^{W,s} \right) \\ &+ \sum_{i \in \Omega^{KCS}} \xi_{w,u,i,y} \cdot max \left(0, P_{i,t,y}^{W,s} - P_{i,t,y}^{W} \right) \\ &+ \sum_{i \in \Omega^{KCS}} \xi_{pv,o,i,y} \cdot max \left(0, P_{i,t,y}^{PV} - P_{i,t,y}^{PV,s} \right) \\ &+ \left. \sum_{i \in \Omega^{KCS}} \xi_{pv,u,i,y} \cdot max \left(0, P_{i,t,y}^{PV,s} - P_{i,t,y}^{PV} \right) \right\} \end{aligned} \tag{17}$$

where Ω^{T}, Ω^{Y} and Ω^{GN} are the set of time-intervals, year and grid-connected nodes, respectively; $\pi_{t,y}^{buy}$ and $\pi_{t,y}^{sell}$ are the electricity purchasing price and feed-in tariff, respectively; $\pi_{y}^{MT,ST}$, $\pi_{y}^{MT,W}$, $\pi_{y}^{MT,PV}$ and $\pi_{m,y}^{MT,BESS}$ are the maintenance cost of substation, micro-WT, PV panels and *m*th-type of BESS, respectively; $P_{i,t,y}^{buy}$ and $P_{i,t,y}^{sell}$ denote the electricity purchased from or sold to the utility grid, respectively; $\zeta_{w,o,i,y}$ and $\zeta_{w,u,i,y}$ are the overestimated and underestimated penalty costs of wind power, respectively; $\zeta_{pv,o,i,y}$ and $\zeta_{pv,u,i,y}$ indicate the overestimated and underestimated penalty costs of solar power; $P_{i,t,y}^{PV}$ and $P_{i,t,y}^{W}$ are the actual available solar and wind power, respectively; $P_{i,t,y}^{PV,s}$ and $P_{i,t,y}^{W,s}$ are the scheduled (predicted) solar and wind power, respectively. Note that the nonlinear penalty terms can be linearized by piecewise linearization method.

The environmental penalty cost is introduced to limit the amount of carbon emissions during the normal operation of power system. In the EVCS-WPE-SLBs system, the primary sources of environmental carbon emissions are the electricity purchased from the utility grid, which is generated by nonrenewable resources. Apart from that, we assume that the process of disposing of retired batteries will also generate some emissions.

$$C_{total}^{envir} = C_{ST}^{envir} + C_{BESS,retire}^{envir}$$

$$= \pi_y^{envir} \sum_{y\in\Omega^Y} \sum_{t\in\Omega^T} \left\{ \sum_{i\in\Omega^{GN}} P_{i,t,y}^{buy} \cdot \delta_y^{ST} \Delta t + \sum_{m\in\Omega^{BESS}} \sum_{i\in\Omega^{KCS}} \lambda_{m,i,y}^{BESS,retire} \cdot \delta_y^{ST} \right) \Bigg\} \quad (18)$$

where π_y^{envir} is the carbon cost coefficient, δ_y^{ST} is the carbon emission intensity of the substation when purchasing electricity; δ_y^{BESS} represents the carbon emission intensity for the retirement of BESS, respectively.

The following constraints are considered in the proposed optimization problem.

$$S_{ij,t,y} + \sum_{i\in\Omega^{GN}} \left(P_{i,t,y}^{buy} - P_{i,t,y}^{sell}\right) + \sum_{i\in\Omega^{KCS}} \left(P_{i,t,y}^{PV}\lambda_{i,y}^{PV} + P_{i,t,y}^{W}\lambda_{i,y}^{W}\right) = \sum_{i\in\Omega^{KCS}} \left[\left(P_{m,i,t,y}^{cha} - P_{m,i,t,y}^{dis}\right)\lambda_{m,i,y}^{BESS} + P_{i,t,y}^{EV}\lambda_i^{CS}\right] + P_{i,t,y}^{L} \forall t \in \Omega^T, ij \in \Omega^{DL}, y \in \Omega^Y \quad (19)$$

$$S_{ij,t,y} - B_{ij}(\theta_{i,t,y} - \theta_{j,t,y}) = 0 \forall t \in T, ij \in \Omega^{DL}, y \in \Omega^Y \quad (20)$$

$$\underline{S_{ij,t,y}} \le S_{ij,t,y} \le \overline{S_{ij,t,y}} \forall t \in T, ij \in \Omega^{DL}, y \in \Omega^Y \quad (21)$$

$$P_{i,t,y}^{PV,s} = (I_{i,t,y}^r / I_{ref}^r) \times P_r^{PV} \times \eta_{PV} \times [1 - \beta_T \times (T_{i,t,y}^C - T_{ref}^C)] \forall t \in \Omega^T \quad (22)$$

$$T_C = T_{amb} + (CT - 20) \times I_{i,t,y}^r / 800 \forall t \in \Omega^T \quad (23)$$

$$P_{i,t,y}^{W,s} = \begin{cases} 0, V_{i,t,y} < v_{in}, V_{i,t,y} > v_{out} \\ a \cdot V_{i,t,y} + b, v_{in} \le V_{i,t,y} \le v_r \\ w_r, v_r < V_{i,t,y} \le v_{out} \end{cases}, \forall i \in \Omega^{KCS}, t \in T, y \in \Omega^Y \quad (24)$$

$$N_{i,y}^{PV} \le \overline{N_{i,y}^{PV}} \times \lambda_{i,y}^{PV} \forall i \in \Omega^{KCS}, y \in \Omega^Y \quad (25)$$

$$N_{i,y}^{W} \le \overline{N_{i,y}^{W}} \times \lambda_{i,y}^{W} \forall i \in \Omega^{KCS}, y \in \Omega^Y \quad (26)$$

where Ω^{DL} is the set of lines; $S_{ij,t,y}$ is the power flow from bus i to bus j; $P_{i,t,y}^{EV}$ and $P_{i,t,y}^{L}$ are the EV charging demand and base load demand at candidate bus i, respectively; B_{ij} and $\theta_{i,t,y}$ are respectively the line susceptance of branch ij and the bus angle; $I_{i,t,y}^r$, T_c, T_{amb}, η_{PV} and β_T represent the solar radiation, cell temperature of PV, ambient temperature, generation efficiency and temperature coefficient of PV, respectively; I_{ref}^r is $1000 W/m^2$. Equations (19)–(21) represent the nodal power balance, power flow constraints and maximum power flow limit, respectively. Equations (22)–(26) are the constraints for PVs and micro-WTs, where $a = w_r/(v_r\text{-}v_{in})$, $b = (\text{-}v_{in}\cdot w_r)/(v_r\text{-}v_{in})$; $V_{i,t,y}$, v_r, v_{in}, v_{out}, w_r are the wind speed, the rated speed, the cut-in speed, cut-out speed, and the power output for the rated speed, respectively.

$$\lambda_{i,t,y}^{ST,buy} + \lambda_{i,t,y}^{ST,sell} \le 1 \forall i \in \Omega^{GN}, t \in \Omega^T, y \in \Omega^Y \quad (27)$$

$$0 \le P_{i,t,y}^{buy} \le \overline{P_{i,t,y}^{buy}} \times \lambda_{i,t,y}^{ST,buy} \forall i \in \Omega^{GN}, t \in \Omega^T, y \in \Omega^Y \quad (28)$$

$$0 \le P_{i,t,y}^{sell} \le \overline{P_{i,t,y}^{sell}} \times \lambda_{i,t,y}^{ST,sell} \forall i \in \Omega^{GN}, t \in \Omega^T, y \in \Omega^Y \quad (29)$$

Grid-connected transaction models are presented in (27)–(29). These models limit the simultaneous process of buying and selling electricity, and also define the upper bound for the amount of power exchanged with the utility grid.

Equations (30)–(45) are the constraints related to BESS and the echelon utilization of SLBs. Furthermore, the decision to install PVs, micro-WTs and BESSs at node i must also satisfy the constraints (11)–(13) related to the fuzzy system results.

$$E_{m,i,t+1,y}^{BESS} = E_{m,i,t,y}^{BESS} + (P_{m,i,t,y}^{cha}\eta_{m,i}^{cha})\Delta t - (P_{m,i,t,y}^{dis}/\eta_{m,i}^{dis})\Delta t \quad (30)$$

$$\underline{E_{m,i,t,y}^{BESS}} \le E_{m,i,t,y}^{BESS} \le (\overline{E_{m,i,t,y}^{BESS}})(\lambda_{m,i,y}^{BESS} - \lambda_{m,i,y}^{BESS,retire}) \quad (31)$$

$$0 \le P_{m,i,t,y}^{dis} \le \overline{P_{m,i,t,y}^{dis}} \times \mu_{m,i,t,y}^{dis} \forall i \in \Omega^{KCS}, t \in \Omega^T, y \in \Omega^Y \quad (32)$$

$$0 \le P_{m,i,t,y}^{cha} \le \overline{P_{m,i,t,y}^{cha}} \times \mu_{m,i,t,y}^{cha} \forall i \in \Omega^{KCS}, t \in \Omega^T, y \in \Omega^Y \quad (33)$$

$$\mu_{m,i,t,y}^{dis} + \mu_{m,i,t,y}^{cha} \le 1 \forall i \in \Omega^{KCS}, t \in \Omega^T, y \in \Omega^Y \quad (34)$$

$$\mu_{m,i,t,y}^{dis} \le \lambda_{m,i,y}^{BESS} \forall i \in \Omega^{KCS}, t \in \Omega^T, y \in \Omega^Y \quad (35)$$

$$\mu_{m,i,t,y}^{cha} \le \lambda_{m,i,y}^{BESS} \forall i \in \Omega^{KCS}, t \in \Omega^T, y \in \Omega^Y \quad (36)$$

$$\lambda_{m,i,y}^{BESS} \le \lambda_{m,i,y+1}^{BESS} \forall i \in \Omega^{KCS}, y \in \Omega^Y \quad (37)$$

$$\lambda_{m,i,y}^{BESS,retire} \le \lambda_{m,i,y+1}^{BESS,retire} \forall i \in \Omega^{KCS}, y \in \Omega^Y \quad (38)$$

$$\lambda_{m,i,y}^{BESS,retire} \le \lambda_{m,i,y}^{BESS} \forall i \in \Omega^{KCS}, y \in \Omega^Y \quad (39)$$

$$0 \le \sum \lambda_{m,i,y}^{BESS} \le 1 \forall i \in \Omega^{KCS}, y \in \Omega^Y \quad (40)$$

$$\Delta DOD_{m,i,t,y} = \left| \frac{E_{m,i,t+1,y}^{BESS} - E_{m,i,t,y}^{BESS}}{E_{m,i,t,y,rated}^{BESS} \times \overline{SOC}} \right| \forall i \in \Omega^{KCS}, t \in \Omega^T, y \in \Omega^Y \quad (41)$$

$$N_{100,m,i,y}^{eqv,day} = \sum_{t\in\Omega^T} N_0 (\Delta DOD_{m,i,t,y})^{k_p} \forall i \in \Omega^{KCS}, y \in \Omega^Y \quad (42)$$

$$Loss_{m,i}^{cycle}(\%) = \left(\sum_{y\in\Omega^Y} N_{days} N_{100,m,i,y}^{eqv,day} \right) N_{100,m,i}^{total} \times 100\% \forall i \in \Omega^{KCS}, y \in \Omega^Y \quad (43)$$

$$SOH_{m,i}(\%) = SOH_{m,i}^{initial}(\%) - Loss_{m,i}^{cycle}(\%) \forall i \in \Omega^{KCS} \tag{44}$$

$$\underline{SOH_{m,i}(\%)} \le SOH_{m,i}(\%) \le \overline{SOH_{m,i}(\%)} \forall i \in \Omega^{KCS} \tag{45}$$

Equation (30) describes the charging and discharging process of the BESS. Equations (31)–(33) respectively limit the electricity stored, the discharging power and the charging power of the BESS. Equations (34)–(36) define two binary decision variables $\mu_{m,i,t,y}^{cha}$ and $\mu_{m,i,t,y}^{dis}$ that ensure the BESS cannot be charged or discharged simultaneously. Equations (37)–(39) ensure that each type of BESS (whether fresh or SLBs) cannot be repeated installed or uninstalled, and a BESS can only be retired after installation. Equation (40) indicates that at the same candidate bus, only the same type of BESS is allowed to install. The time-series expression describing the change of DOD, $\Delta DOD_{m,i,t,y}$, is given in (41). Equation (42) gives the definition for the 100%-DOD equivalent BESS daily cycle number $N_{100,m,i,y}^{eqv,day}$, where N_0 and k_p are battery cycle parameter and Peukert lifetime constant, respectively. The loss of mth-type BESS cycles $Loss_{m,i}^{cycle}(\%)$ and the real-time remaining state-of-health $SOH_{m,i}$ (%) are respectively calculated by (43) and (44). Equation (45) strictly limits the real-time remaining SOH value $SOH_{m,i}$ (%) within the range of maximum and minimum allowable SOH depends on the types of BESS. (Note that fresh and SLBs have different allowable SOH boundaries). The safety margin for the BESS is set to a limit, and the charging or discharging behaviors are constrained when the remaining health status is low. Note that the SLB models in our article are constrained by their SOH, which is the most common approach to limiting the operation of SLBs [1], [26], [27]. The detailed mathematical modeling of SLBs is outside the scope of our study.

V. Case Study

In this article, the IEEE 33-bus distribution system coupled with a 25-node transportation network is used to illustrate the proposed planning method. The simulations were conducted using MATLAB on a 64-bit laptop with 2.60 GHz CPU and 16GB RAM. The proposed optimization model is solved by SCIP of the OPTI toolbox in MATLAB. SCIP is a powerful solver that employs sophisticated strategies (e.g., branch-and-bound, cutting planes, and primal heuristics) to find solutions, especially useful for mixed-integer problems. The optimality gap (BBGap) values for our cases are all extremely close to zero, indicating strong convergence to the global optimum.

A. Test System and Parameters Settings

The coupled relationship between the distribution system and transportation system is illustrated in Fig. 5. We assume that the planner is a social planner and has access to all the required parameters of the system. This is a reasonable assumption as the planning of the EVCS-WPE-SLBs is considered a regional project with the goal to achieve social welfare. The decimal next to each node indicates the node's weight, while the integer represents the number of EVs at that node. It is important to note

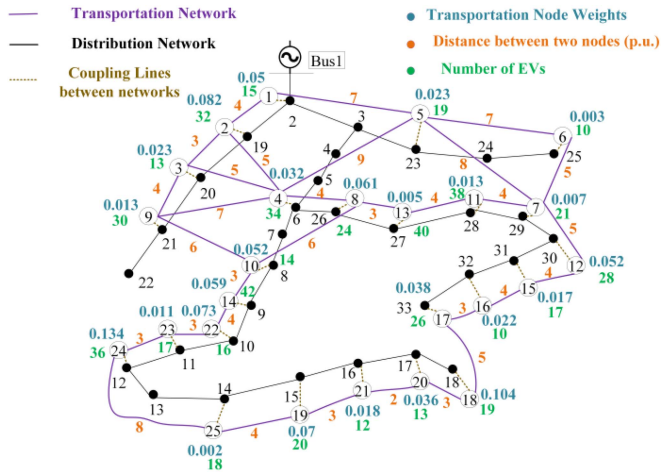

Fig. 5. Coupled 33-buses distribution network used for case studies.

that the node weight represents a measure of the traffic volume or passenger flow at a particular node in the transportation network. The number on each arc represents the distance in p.u. between two connected nodes. We assume that the demand at each transportation node is supplied by its nearest distribution bus.

The total planning period of the system is 5 years. The base demand and electricity prices are obtained from the historical data of Australian Energy Market Operator (AEMO) [28]. The solar radiation, wind speed and ambient temperature are gathered from the historical data of Australian Bureau of Meteorology [29]. Detailed system parameter configurations and costs of BESS and renewable energy facilities are quoted from [7], [30], including the capacity, charging/discharging power, efficiency, SOH of BESS, fixed investment cost, operation and maintenance cost, carbon cost coefficient, etc. The battery cycle parameter N_0 and Peukert lifetime constant K_p are set to 1. The temperature coefficient β_T, cell reference temperature T_{ref}^C and normal operation cell temperature CT are 0.0045, 25 °C, and 55 °C, respectively. The cut-in speed, cut-out speed, rated speed and rated power of the micro-WT are 3 m/s, 25 m/s, 11 m/s and 10 kW, respectively. The interest rate is set to be 3%. To satisfy the EV's charging needs, we assume the construction of 6 charging stations. Some necessary values for FISs of some typical nodes are given in Fig. 6.

B. Numerical Results and Analysis

Three cases are conducted to demonstrate the economic benefits of the SLBs in the EVCS-WPE-SLBs system.

Case1: The BESS is considered to be composed of fresh batteries or SLBs simultaneously.

Case2: The BESS is only composed of fresh batteries.

Case3: The BESS is only composed of SLBs.

Case 1 is selected as the base case to verify whether the proposed planning method can reasonably make the trade-off between the selection of fresh batteries and SLBs. Case 2 and 3 are conducted to show the difference in different types of cost.

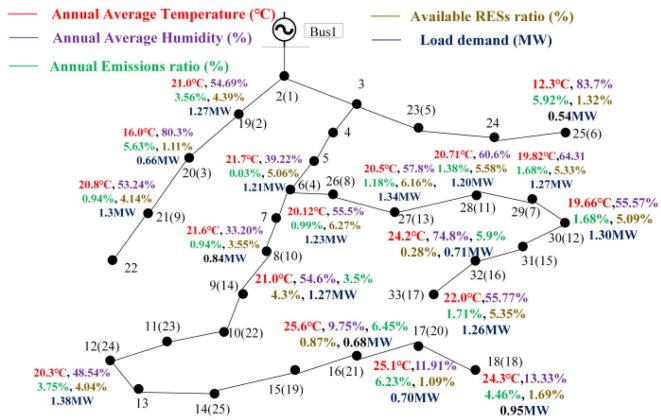

Fig. 6. Some necessary values for the FIS of some typical nodes.

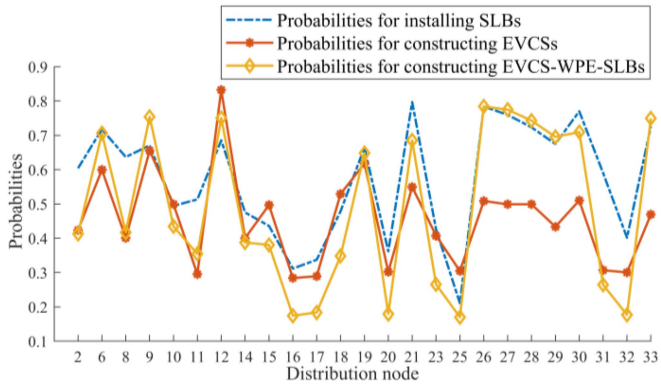

Fig. 7. Results of the fuzzy inference system.

TABLE IV
RESULTS OF DIFFERENT CASES

Case	Total Cost (M$)	Locations (Bus number)	BESS Investment (%)	RES Installation	BESS O&M cost (%)
1	5.6067	6, 12, 19, 21,27,33	100%	325 PV 193 micro-WTs	100%
2	5.6335	6, 12, 19, 21,27,33	274.7%	356 PVs 142 micro-WTs	58.82%
3	5.6166	6, 9, 12, 21,27,33	54.07%	318 PVs 207 micro-WTs	105.88%

Fig. 7 illustrates the three probability sets obtained by the proposed method. In this article, the 11 nodes with the highest probability are selected as the candidate node set, and therefore, Ω^{KCS} consists of bus {6, 9, 12, 19, 21, 26, 27, 28, 29, 30, 33}. Note that the performance of the FIS is related to the choice of the parameters. We have used the cross-validation method and carried out a sensitivity analysis to assess and improve our FIS model. By varying the parameters (e.g., MFs and fuzzy rules) within a reasonable range, we have studied the effects of these variations on the output of our FIS. This has allowed us to understand the system resilience to changes in parameters, and ensure our results are realistic.

The results of the different cases are summarized in Table IV. According to the results of case 1, 6 charging stations are built at distribution bus 6, 12, 19, 21, 27, 33; 247 and 78 PV panels are installed respectively at bus 21 and 27; 193 micro-WTs are built at bus 12, 19, 21, 27 and 33. Besides, the system installed BESS composed of fresh batteries at bus 33 in the second year and BESS composed of SLBs at bus 19 in the fourth year. The BESSs installed in the remaining nodes are all composed of SLBs. According to the results, the operation of the BESS is obviously constrained by the SOH safety margin. If the SOH value falls below the minimum safety operation margin, the BESS will be replaced by the new one, either fresh or SLBs to ensure the reliable operation of the system.

Compared to the $5.6335 million of case 2 and $5.6166 million of case 3, the total cost of case 1 is the lowest with about $5.6067 million. This disparity arises because the BESSs in case 2 are all composed of fresh batteries, resulting in the highest initial investment cost of BESS among the three cases (around 274.7% of the base case). However, the maintenance cost is also the lowest, which is only 58.82% of that in case 1. On the other hand, the investment cost of the BESS in case 3 is the lowest among all cases at roughly 54.07% of the base case, while its operation and maintenance cost is the highest at about 105.88% of the base case. Although there is an increase in the investment and maintenance costs of renewable energy facilities in case 3, its total cost remains lower than case 2 due to the substantial lower investment cost of SLBs. In summary, it can be concluded that Case 1 combines the advantages of the other cases. It significantly reduces the investment cost of BESS, and the remaining system costs are not much different from others, thereby greatly reducing the total system cost.

The comparison of the operation of the EVCS-WPE-SLBs system in the fourth year of the three cases is illustrated in Fig. 8. As can be seen, almost all demands in the daytime are supplied by solar and wind power, and excess energy generated is used to charge the BESS or is fed back to the grid to earn profit. From a long-term perspective, using RES-based generation is a better choice in terms of economic benefits and environmental protection compared to purchasing electricity from the utility grid. Besides, since solar radiation rises in the morning, decreases in the afternoon and drops to zero at night, the output of PVs similarly increases over time, peaks at noon, and then gradually declines to zero. When there is no output of PVs in the evening, the BESS begins to discharge, together with the microturbines and the purchased electricity to supply the demands. The result shows the advantages of the EVCS-WPE-SLBs system. On one hand, the system can be supplied by RES and BESS for most of the day, considerably reducing the carbon emissions and pollutants. On the other hand, BESS can store excess electricity generated during low-demand or low-price periods, and discharge it during peak hours or high-price periods, thus mitigating the impact of price fluctuations in the electricity market.

C. Comparative Analysis of the Proposed Method

In order to analyze the effectiveness of the proposed FIS-based planning framework, some comparative cases are studied.

Case4: Similar to case 1, but the FIS-based candidate node set selection method is not applied. In this case, the utilization

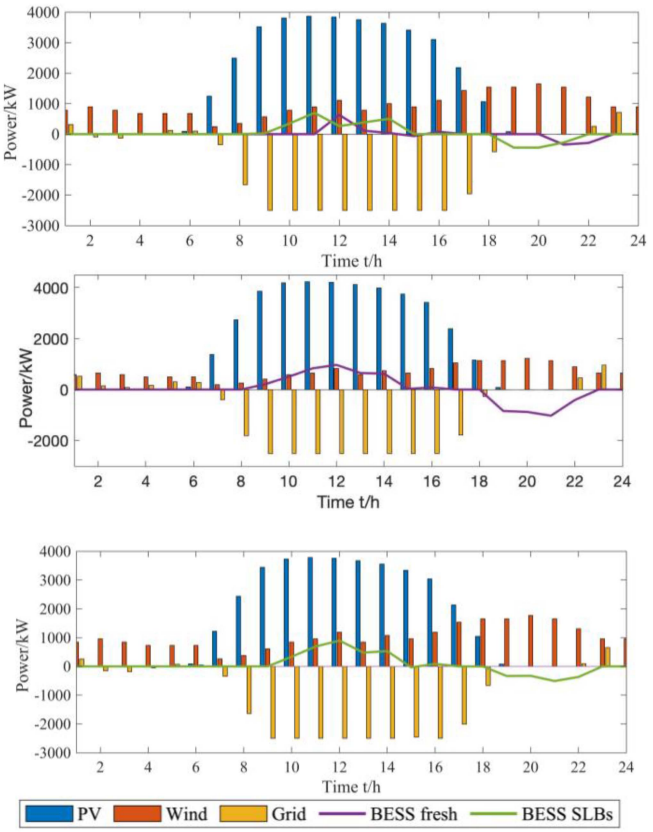

Fig. 8. Optimization results of different cases.

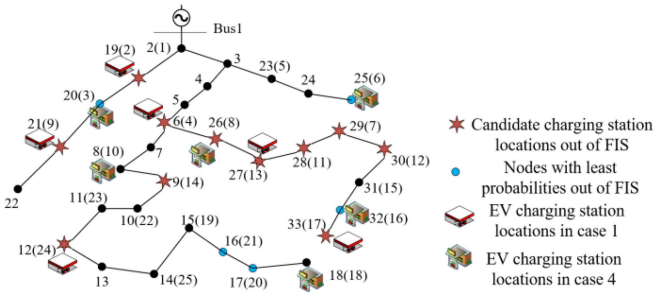

Fig. 9. Comparison of the location of case 1 and case 4.

requirements of the SLBs and the transportation system features are ignored.

As can be seen in Fig. 9, in Case 1, where the proposed FIS-based planning framework is applied, EVCSs are constructed at locations with mild temperature (bus 6, bus 19, bus 33), proper humidity (bus 12, bus 19, bus 21), low environmental pollution levels (bus 6, bus 27, bus 33), high node weights (bus 12, bus 19), large number of EVs (bus 6, bus 12, bus 27), large distances between neighboring nodes (bus 6, bus 12, bus 21), abundant renewable energy resources (bus 6, bus 27, bus 33), large demand levels (bus 12, bus 19, bus 21, bus 27, bus 33). However, in Case 4, where the proposed framework is not applied, only 1 out of the 11 nodes with the highest probability are selected for EVCS construction, and even 3 of the 5 nodes with the lowest probabilities are selected. For instance, the EVCS-WPE-SLBs systems are constructed on the nodes where the humidity is high

TABLE V
COMPARISON OF CASE 1 AND CASE 4

		Case 1		Case 4	
Variables	Total	4725		12447	
	BESS	3278		9834	
	RESs	572		1716	
	Others	875		897	
Constraints		inequality	equality	inequality	equality
	Total	3394	1915	6870	4159
	BESS	3190	1078	6402	3234
	Others	204	837	468	925

(83.70% at node 25 and 80.03% at node 20), the available RESs ratio is low (0.28% at node 32) and the demand is low (0.54 MW at node 25 and 0.66 MW at node 20). However, these results are obviously not realistic and re-adjustment is needed in the future according to actual system conditions in real life.

Table V compares the total number of variables and constraints for one year in these two cases, particularly focusing on the BESS and RESs. Note that the "BESS" category of the constraints includes daily operational constraints (30)–(36), changes in DOD (41), and equivalent BESS daily cycle number (42). The "others" category in the table includes power flows (19)–(20), the grid transaction (27)–(29), the loss of BESS life cycles (43) and real-time remaining SOH (44) in one planning period. As can be seen from Table V, the number of variables to be optimized is 12447 in case 4. As a comparison, in case1, where a narrowed candidate node set obtained by our proposed method is applied, the number of variables reduces significantly to 4725. Correspondingly, the number of constraints drastically drops from 11029 in total to 5309. Moreover, case 1 is 5.32 times faster than that of case 4, demonstrating a significant reduction in execution time. Therefore, it is evident that the search space is reduced and the computational time is shortened.

Furthermore, the planning of the EVCS-WPE-SLBs system typically poses large-scale problems in practice. The problem becomes extremely complex when the locations of EVCSs is unrestricted within the network. Therefore, limiting the set of potential locations is obviously advantageous for optimizing such large-scale tasks.

It is important to note that the use of our proposed method into the planning of EVCS-WPS-SLBs system in reality may require collaboration and data exchange across various systems. For example, it might necessitate data from transportation systems (such as the traffic flow and the distance between nodes), power grid system (like demand and maximum power system capacity in the area), and meteorological department (like solar radiation and wind speed). However, such a situation is quite common in developing countries, where public infrastructures are constructed by the government. This centralized planning approach, promotes effective inter-departmental data sharing for strategic planning.

Figs. 10 and 11 show the comparison of the results obtained by the FIS, Random Forest, and KNN under the same rules

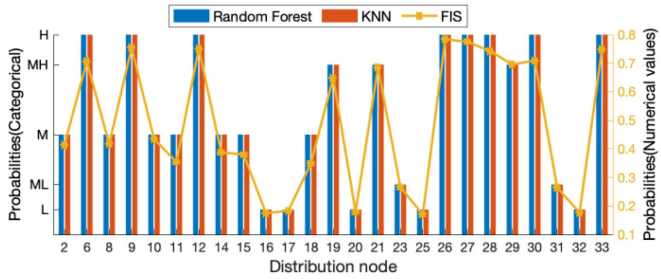

Fig. 10. Comparison of different methods (1).

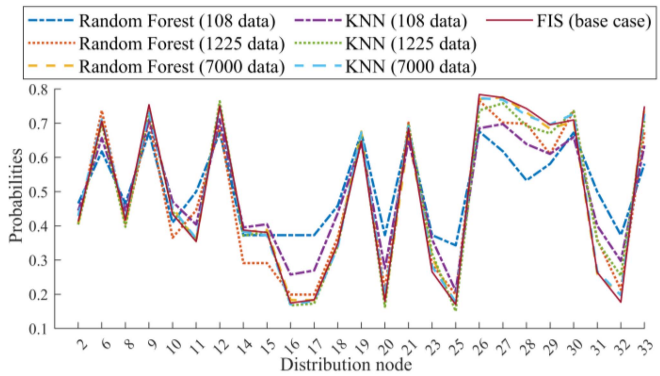

Fig. 11. Comparison of different methods (2).

table or using the same generated dataset. When the inputs are in categorical (e.g., Low, Medium and High), as illustrated in Fig. 10, the crisp values obtained by FIS are extremely helpful for decision-making. This provides more precise and accurate results compared to the categorical results from the other two methods. Moreover, unlike many other machine learning methods, a FIS does not need a huge amount of data to be trained. This is especially useful when data collection is difficult. As illustrated in Fig. 11, the accuracy of both random forest and KNN methods is highly sensitive to the amount of data used for training. The greater the amount of data used for training, the more precise the results obtained. Additionally, after training with 7000 sets of data, the maximum error between the results obtained by FIS and those obtained by the other two methods does not exceed 1%. In summary, the FIS has the advantage of generating crisp values for decision-making from categorical inputs, which may not be as effectively handled by other methods. Additionally, the FIS allows the incorporation of prior knowledge in the form of fuzzy rules, which is particularly preferable in scenarios where the data is unavailable or difficult to obtain.

D. Scalability Analysis of the Proposed Method

In practical planning applications, the impact of each factor among all factors on the planning result may not be evenly distributed. In other words, a factor may be prioritized during the planning process. The joint effect under different prioritized factors on the probability of constructing the EVCS-WPE-SLBs at each node is illustrated in Fig. 12. Note that the contribution of each factor to the final result is determined by membership

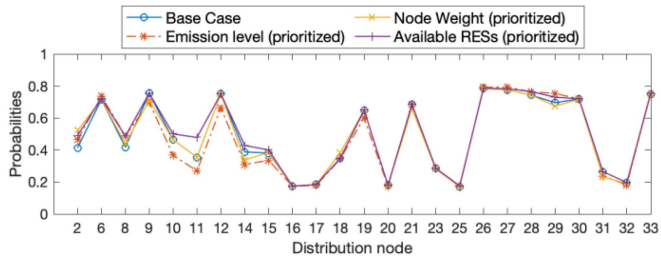

Fig. 12. Results on different priorities of off-site factors.

degrees and fuzzy rules. By modifying the MFs of each input and rules table (Tables I, II and III), different factors can be assigned different priorities.

As illustrated in Fig. 12, the top five candidate nodes with the highest probability of constructing the EVCS-WPE-SLBs vary when different off-site factors are prioritized. For example, when the emission level is prioritized, the top five distribution nodes are bus {27, 26, 28, 29, 33}. However, when node weight and the amount of RESs are prioritized, the top five distribution nodes consist of bus {26, 27, 12, 33, 28} and bus {26, 27, 28, 33, 9}, respectively.

Furthermore, for those buses (such as bus 10 and bus 11) with a relatively high emission level (which implies less suitability for the utilization of SLBs at that location) but relatively high available renewable energy resources (which implies greater suitability for the EVCS-WPE-SLBs system), the probability of constructing EVCS-WPE-SLBs at these nodes is low when the emission level is prioritized (about 0.3668 for bus 10 and 0.2689 for bus 11), but high when the amount of RESs is prioritized (around 0.5011 for bus 10 and 0.4780 for bus 11). Moreover, as can be seen from Fig. 12, regardless of which of these factors predominates, there are no significant differences in the results for some nodes. This is because among these nodes, some already have high emission levels and low available RESs (such as bus 16, 17, 20, 25, 32), and some already have low emission levels and a high amount of RESs (such as buses 21, 26-30, 33). Therefore, the prioritization of these factors does not significantly influence the probabilities for the construction of EVCS-WPE-SLBs at these nodes.

The results indicate that the proposed method is versatile and adaptable. It effectively accounts for the varying priorities of different off-site factors during the planning process. Its ability to adjust to varying factor priorities makes the method particularly suitable for practical planning applications, offering customized and optimized planning solutions based on the specific factor priorities.

VI. Conclusion

This article proposes a novel fuzzy inference system (FIS) based planning framework for EV charging stations which considers wind power, PV power, BESS and the utilization of second-life batteries (EVCS-WPE-SLBs system). In this framework, a narrowed and the most probable candidate node set for EVCS-WPE-SLBs system is obtained with the consideration of several off-site factors which jointly determine the optimal

planning results, including the installation and utilization requirements of SLBs, the features of transportation network and power system properties. A probability set for the most suitable locations to utilize SLBs in the system and a probability set for locating the EVCSs most properly in a transportation network are first obtained by two independent FIS. Then, by combining additional information about available RES and load demand of each node, a narrowed and most probable candidate set for EVCS-WPE-SLBs system is determined. Numerical case studies are conducted on a coupled 33-bus distribution system and 25-bus transportation system to demonstrate the proposed planning method. Two key conclusions are obtained: 1) The reasonable utilization of SLBs in the EVCS-WPE-SLBs system can reduce the cost of the system while maintaining the normal and flexible operation condition of the system. 2) A narrowed candidate node set among all system nodes can be easily obtained by employing the proposed FIS method, which can not only simplify the optimization problem, the results obtained are more practical according to actual system operation conditions.

REFERENCES

[1] J. Li, S. He, Q. Yang, Z. Wei, Y. Li, and H. He, "A comprehensive review of second life batteries towards sustainable mechanisms: Potential, challenges, and future prospects," *IEEE Trans. Transp. Electrific.*, early access, Nov. 14, 2022, doi: 10.1109/TTE.2022.3220411.

[2] S. Jiang, L. Zhang, H. Hua, X. Liu, H. Wu, and Z. Yuan, "Assessment of end-of-life electric vehicle batteries in China: Future scenarios and economic benefits," *Waste Manage.*, vol. 135, pp. 70–78, Nov. 2021.

[3] V. V. Viswanathan and M. Kintner-Meyer, "Second use of transportation batteries: Maximizing the value of batteries for transportation and grid services," *IEEE Trans. Veh. Technol.*, vol. 60, no. 7, pp. 2963–2970, Sep. 2011.

[4] E. Hossain, D. Murtaugh, J. Mody, H. M. R. Faruque, M. S. H. Sunny, and N. Mohammad, "A comprehensive review on second-life batteries: Current state, manufacturing considerations, applications, impacts, barriers potential solutions, business strategies, and policies," *IEEE Access*, vol. 7, pp. 73215–73252, 2019.

[5] L. C. Casals, B. A. García, and C. Canal, "Second life batteries lifespan: Rest of useful life and environmental analysis," *J. Environ. Manage.*, vol. 232, pp. 354–363, Feb. 2019.

[6] D. Strickland, L. Chittock, D. A. Stone, M. P. Foster, and B. Price, "Estimation of transportation battery second life for use in electricity grid systems," *IEEE Trans. Sustain. Energy*, vol. 5, no. 3, pp. 795–803, Jul. 2014.

[7] Y. Yang, J. Qiu, C. Zhang, J. Zhao, and G. Wang, "Flexible integrated network planning considering echelon utilization of second life of used electric vehicle batteries," *IEEE Trans. Transp. Electrif.*, vol. 8, no. 1, pp. 263–276, Mar. 2022.

[8] I. Mathews, B. Xu, W. He, V. Barreto, T. Buonassisi, and I. M. Peters, "Technoeconomic model of second-life batteries for utility-scale solar considering calendar and cycle aging," *Appl. Energy*, vol. 269, Jul. 2020, Art. no. 115127.

[9] J. Neubauer, K. Smith, E. Wood, and A. Pesaran, "Identifying and overcoming critical barriers to widespread second use of PEV batteries," Nat. Renewable Energy Lab., Golden, CO, USA, Tech. Rep. NREL/TP-5400-63332, 2015.

[10] J. Ugirumurera and Z. J. Haas, "Optimal capacity sizing for completely green charging systems for electric vehicles," *IEEE Trans. Transp. Electrif.*, vol. 3, no. 3, pp. 565–577, Sep. 2017.

[11] Q. Dai, J. Liu, and Q. Wei, "Optimal photovoltaic/battery energy storage/electric vehicle charging station design based on multi-agent particle swarm optimization algorithm," *Sustainability*, vol. 11, no. 7, pp. 1–21, Apr. 2019.

[12] W. Yao et al., "A multi-objective collaborative planning strategy for integrated power distribution and electric vehicle charging systems," *IEEE Trans. Power Syst.*, vol. 29, no. 4, pp. 1811–1821, Jul. 2014.

[13] B. Sun, "A multi-objective optimization model for fast electric vehicle charging stations with wind, PV power and energy storage," *J. Cleaner Prod.*, vol. 288, pp. 1–17, Mar. 2021.

[14] F. Xu, J. Liu, S. Lin, Q. Dai, and C. Li, "A multi-objective optimization model of hybrid energy storage system for non-grid-connected wind power: A case study in China," *Energy*, vol. 163, pp. 585–603, Nov. 2018.

[15] R. Jing, J. Wang, N. Shah, and M. Guo, "Emerging supply chain of utilising electrical vehicle retired batteries in distributed energy systems," *Adv. Appl. Energy*, vol. 1, 2021, Art. no. 100002.

[16] K. Gur, D. Chatzikyriakou, C. Baschet, and M. Salomon, "The reuse of electrified vehicle batteries as a means of integrating renewable energy into the European electricity grid: A policy and market analysis," *Energy Policy*, vol. 113, pp. 535–545, Feb. 2018.

[17] Y. Deng, Y. Zhang, F. Luo, and G. Ranzi, "Many-objective HEMS based on multi-scale occupant satisfaction modelling and second-life BESS utilization," *IEEE Trans. Sustain. Energy*, vol. 13, no. 2, pp. 934–947, Apr. 2022.

[18] Y. Zhang, Y. Xu, H. Yang, Z. Y. Dong, and R. Zhang, "Optimal whole-life-cycle planning of battery energy storage for multi-functional services in power systems," *IEEE Trans. Sustain. Energy*, vol. 11, no. 4, pp. 2077–2086, Oct. 2020.

[19] Y. Deng, Y. Zhang, F. Luo, and Y. Mu, "Operational planning of centralized charging stations utilizing second-life battery energy storage systems," *IEEE Trans. Sustain. Energy*, vol. 12, no. 1, pp. 387–399, Jan. 2021.

[20] G. Graber, V. Galdi, V. Calderaro, and P. Mancarella, "A stochastic approach to size EV charging stations with support of second life battery storage systems," in *Proc. IEEE Manchester PowerTech*, 2017, pp. 1–6.

[21] O. Erdinc, B. Vural, and M. Uzunoglu, "A wavelet-fuzzy logic based energy management strategy for a fuel cell/battery/ultra-capacitor hybrid vehicular power system," *J. Power Sources*, vol. 194, no. 1, pp. 369–380, Oct. 2009.

[22] I. Krashenyi, J. Ramírez, A. Popov, and J. Manuel Górriz, "Fuzzy computer-aided Alzheimer's disease diagnosis based on MRI data," *Curr. Alzheimer Res.*, vol. 13, no. 5, pp. 545–556, 2016.

[23] A. Bouallaga, A. Merdassi, A. Davigny, B. Robyns, and V. Courtecuisse, "Minimization of energy transmission cost and CO2 emissions using coordination of electric vehicle and wind power (W2V)," in *Proc. IEEE Grenoble Conf.*, 2013, pp. 1–6.

[24] K. Zhang, C. Mao, J. Lu, D. Wang, X. Chen, and J. Zhang, "Optimal control of state-of-charge of superconducting magnetic energy storage for wind power system," *IET Renew. Power Gener.*, vol. 8, no. 1, pp. 58–66, Jan. 2014.

[25] T. T. Ku, B. R. Ke, Y. L. Ke, and C. K. Wen, "Application of fuzzy control for smart charging of electric vehicles," in *Proc. IEEE/IAS 53rd Ind. Commercial Power Syst. Tech. Conf.*, 2017, pp. 1–4.

[26] G. He, Q. Chen, C. Kang, P. Pinson, and Q. Xia, "Optimal bidding strategy of battery storage in power markets considering performance-based regulation and battery cycle life," *IEEE Trans. Smart Grid*, vol. 7, no. 5, pp. 2359–2367, Sep. 2016.

[27] D. Tran and A. M. Khambadkone, "Energy management for lifetime extension of energy storage system in micro-grid applications," *IEEE Trans. Smart Grid*, vol. 4, no. 3, pp. 1289–1296, Sep. 2013.

[28] Australian Energy Market Operator (AEMO). Accessed: Nov. 1, 2022. [Online]. Available: http://www.aemo.com.au/

[29] Australian Government Bureau of Meteorology. Accessed: Nov. 1, 2022. [Online]. Available: http://www.bom.gov.au/

[30] C. Zhang, J. Qiu, Y. Yang, and J. Zhao, "Trading-oriented battery energy storage planning for distribution market," *Int. J. Elect. Power Energy Syst.*, vol. 129, Jul. 2021, Art. no. 106848.

Jiafeng Lin received the B.Eng. degree in electrical engineering and automation from the Fujian University of Technology, Fuzhou, China in 2020, and the M.E. degree in electrical engineering in 2022 from The University of Sydney, Sydney, NSW, Australia, where he is currently working toward the Ph.D. degree in electrical engineering. His research interests include power system operation and planning, electrical vehicles, and renewable energy integration.

Jing Qiu (Senior Member, IEEE) received the B.Eng. degree in electrical and control engineering from Shandong University, Jinan, China, in 2008, the M.Sc. degree in environmental policy and management, majoring in carbon financing in the power sector from The University of Manchester, Manchester, U.K., in 2010, and the Ph.D. degree in electrical engineering from the University of Newcastle, Callaghan, NSW, Australia, in 2014. He is currently a Senior Lecturer of electrical engineering with The University of Sydney, Sydney, NSW. His research interests include power system planning, data-driven energy market analysis, and artificial intelligence (AI)-assisted energy pricing and trading strategies. He is an Editorial Board Member of *IET Renewable Power Generation* and *Energy Conversion and Economics*.

Yi Yang (Graduate Student Member, IEEE) received the B.Eng. degree in electrical engineering and automation from the Xiamen University of Technology, Xiamen, China in 2017, and the M.P.Ed. degree in electrical engineering in 2020 from The University of Sydney, Sydney, NSW, Australia, where he is currently working toward the Ph.D. degree in electrical engineering. His research interests include power system planning, low-carbon economy, electric vehicles, and electricity market.

Weidong Lin received the M.E. degree in mechanical and electrical engineering from Chongqing Architectural Engineering College (now Chongqing University), Chongqing, China, in 1992. He is currently a professional Senior Engineer with the Fujian Provincial Institute of Architectural Design and Research Company Ltd., Fuzhou, China. His research interests include power distribution and supply, architectural electrical engineering, and solar photovoltaic power generation.